



Leveraging a Dynamic Differential Annealed Optimization and Recalling Enhanced Recurrent Neural Network for Maximum Power Point Tracking in Wind Energy Conversion System

P. Rajesh¹ · S. Muthubalaji² · S. Srinivasan² · Francis H Shajin³

Received: 27 October 2020 / Accepted: 19 April 2022 / Published online: 29 April 2022
© The Author(s), under exclusive licence to Springer Nature Singapore Pte Ltd. 2022

Abstract

In this article, a hybrid strategy is proposed to track that maximum power of Wind Energy Conversion System (WECS). The proposed technique is the joint execution of Dynamic Differential Annealed Optimization (DDAO) and Recalling Enhanced Recurrent Neural Network (RERNN) hence, it is called D²AORERN² approach. In the proposed work, DDAO has input parameters, like rectifier outputs that means rectifier dc voltage, dc current, time. Based on input parameters, Dynamic Differential Annealed Optimization optimizes and minimizes the error in rectifier power and makes training dataset based on maximal power point tracking conditions. Based on accomplished dataset, the RERNN finds the optimal solution. The rectifier's reference dc voltage is transformed for controlling the inverter switch pulses. Finally, the proposed method is activated in MATLAB/Simulink, its superiority is analyzed with various existing methods, like genetic algorithm (GA), particle swarm optimization (PSO), Hill Climb Search (HCS). The efficiency of proposed system is likened to several existing technique as GA, PSO and HCS. The efficiency of GA, PSO, HCS and proposed technique is 81%, 85%, 89% and 99%. Thus the proposed technique achieves best result than the other techniques.

Keywords Maximum power · Wind energy conversion system · DC side voltage · Inverter switches · Control pulses

Introduction

Wind power generation system (WPGS) is utilized for energy supply from remote loads and for autonomous systems associated with grid related applications [22]. The important designing aspect in WPGS is chosen exact turbine power generator engineering [27]. Typically, the technology of changeable speed turbine power generator is preferential likened with continual speed turbine, whereas best voltage, recurrence rate regulations, cutting ideal energy depending on the quality of current atmosphere is provided. [6, 13]. Electrical power

generator is deemed as squirrel cage induction generator or dual fed induction or synchronous generator [3, 8]. Depending on WPGS, electric power production is generally direct by 2 positions: (i) variable, (ii) constant power production ([9, 11, 12]. Constant power production position is generally initialized under wind speed movements at rated speed and it is deactivate if it exceeds the cut-off power value producing mechanism, also it does not maintain shaft turbine speed. It commonly initialized in case of wind speed represents nominal along cut-off value has minimal value associated with WPGS.

Such exacting areas for single value include velocity of wind flow, energy of grabbed wind flow associated with rotor speed. When the rotor is operated at optimal speed, the higher energy is extracted through the flow of wind [10, 31]. MPPT is necessary to related wind power generation [40]. The exacting MPPT method raises the capability of mechanical with electrical power change by regulating the turbine rotor speed with actual flow of wind speed [29, 34, 39]. Nevertheless, the output of WG energy may be mechanically control for changing the blade's inclination angle [26, 35]. It does not cost effective, resulting in a higher-proficiency energy conversion

✉ P. Rajesh
rajeshkannan.mt@gmail.com

¹ Department of Electrical and Electronics Engineering, Anna University, Chennai, India

² Department of Electrical and Electronics Engineering, CMR College of Engineering & Technology, Hyderabad, Telangana, India

³ Department of Electronics and Communication Engineering, Anna University, Chennai, India

rate, so this component emits maximum power as a wind system, and it minimizes the overall cost of the system [28]. Specific MPPT models typically depend on estimation / assessing the velocity of wind flow, measurement / computation of output power, power curves [41]. This is employed in control schemes, such as tip speed ratio, optimal torque, power mapping, disturbance search, surveillance / HCS [30].

The tip speed ratio requires wind speed and rotor speed calculation, which increases performance to preserve expenditure, although power map regulate the power curve of system turbine and its speed still work sluggishly [5, 32]. HCS could also be largest control program that in go round, does not require any previous experience on device that certainly self-governing of turbine aspects, generator, wind; hence it contains few disadvantages for speed compensation as well as bad directionality resulting changing the wind condition [18]. At last, soft computing tactics created as AI is utilized for pattern variance, more over enhance the robustness of dynamic speed control including static [7, 21]. The tactics of feasible scaling strategies utilized at MPPT approaches depend on fuzzy logic, neural networks, particle swarm optimization etc. [1].

Therefore, this article introduces a hybrid approach for tracking the maximum power of WECS. The proposed approach is the combined execution of DDAO and RERNN, thus, it is called $D^2AORERN^2$ approach. In the proposed work, DDAO has input parameters like rectifier outputs such as rectifier dc voltage with current, time. The input parameters based Dynamic Differential Annealed Optimization optimizes and minimizes the error in rectifier power, and makes training dataset based on maximal power point tracking conditions. Based on accomplished dataset, the RERNN finds the optimal solution. Remaining work was organized as: segment 2 presents the recent investigation works, segment 3 explains the proposed method, segment 4 shows the outcomes with discussion, segment 5 presents the conclusion.

Recent Research Work: A Brief Review

Several research works were previously suggested in the literatures depending on MPPT in WECS with various strategies and aspects. A few of them are reviewed here,

Wang et al. [38] have introduced the design of a multivariable super torque control system of WECS based upon doubly fed induction generator (DFIG), accomplish MPPT. Taking into account the complexity of framework and the parameters of non-linear system, the adaptive algorithm was used for suppressing that parametric uncertainty and exterior disturbances successfully in the absence of information of upper limits beforehand. To monitor the optimal powers at finite time, the presented controller was able to achieve the smooth controlling of active with reactive power. Also, a new

Lyapunov function was built to test finite time convergence method. Khan [20] have explained the new Artificial Intelligence-base Adaptive Perturb and observe for actual time MPPT hybrid control to reach the maximal power point of wind turbine system. The presented method was “to enlarge the mathematic computation of control structure, then remove the drawback of typical MPPT along with fuzzy logic control”. At presented system, by utilizing fuzzy logic controller, the optimal disturbance was calculated. This optimal disturbance was introduced in the adaptive P&O system which was the advantageous duty cycle created DC-DC power converter with presented system to accomplish maximal power point tracking and improve the performance of proposed structure. Samokhvalov et al. [33] have suggested the efficiency of WECS on wind speed using the mode of maintaining the maximal power point tracking, which allows maximum power to be removed as wind energy. The provision of optimal turbine rotation speed was calculated using the maximum power mode that was carried out using the vector control system of permanent magnet synchronous generator. The mechanic losses in gearbox and synchronous machine were determined, the losses in the steel of the synchronous machine and the switching losses in an autonomous voltage inverter were taken into account. Eltamaly et al. [14] have illustrated fuzzy logic controller base maximal power point tracking approach of WECS. The efficiency of maximal power point tracking approach was evaluated mathematically and authenticated with the simulation via MATLAB/PSIM/Simulink. The suggested system recovers the speed, accuracy of maximal power point tracking. Also, the simulation outcomes were performed to commend the efficiency of the proposed MPPT approach, and the entire outcomes have totally established the sufficiency of MPPT approach.

Vu et al. [37] have elucidated that the issues in monitoring MPP of WECS was taken in account. Under this article the WECS was concurrently exaggerated via uncertainties and arbitrary disturbance so that WECS more difficult to control. A novel system was implemented for synthesizing a polynomial disturbance viewer to guess the aerodynamic torque, the wind speed and the electromagnetic torque, all these were occurred in the absence of utilizing sensors. Not like earlier techniques, uncertainties and disturbances were approximated and then the estimates of uncertainties and disturbances were transmitted to Linear Quadratic Regulator (LQR) controller. It could be observed that the uncertainties were varying over time and both uncertainties and shocks were not required for fulfilling the limited restrictions. Alzayed et al. [4] have explained a cascaded-forward neural network (CFNN) MPE that preserves the advantages of MPE in addition to provide the flexibility of power output that was considerably less complexity under the control circuit. The presented approach utilizes that cascading- forward neural network to learn that non-linear aerodynamic dynamics of wind turbines and

accomplishes precise power tracking. Also, it reformulates that equation of voltages of d-q axes of machine to work that wind energy conversion systems (WECS) were under optimal conditions by assuming the speed of wind, the temperature of air, the power demand. In addition, it does not necessitate any adjustment process. Tonsing et al. [36] have defined the state-of-art Hill Climb Search (HCS) based MPPT algorithm of WECS. Due to the erratic quality of wind, it was hard for creating the power constantly. Therefore, it was necessary to remove the maximal power as wind obtainable. This may be accomplished with Hill Climb Search algorithm that happens generator to monitor that MPP of WTS in fluctuating and incompatible wind conditions.

Background of the Research Work

The wide range of wind speeds makes the vital energy of the process unequal to increase the defined modes of energy at the point of maximum force. Additionally, maximal aerodynamic proficiency attains to utilizes optimum employment of wind energy to maintenance of path controller. Several kinds of controller for optimum wind energy deletion methods were presented in the literature, like tip-speed ratio controller, power signal feedback, hill climb search. But, these techniques were inferior due to the problem at wind measurements and Turbine speed uniqueness. The artificial intelligence methods are neural and disperse networks were executed with solving estimation problem while utilizing suitable precise model. In the neural network, the observation of the uses of traditional data was complete, also the data obtains for the operation of the system. Therefore, a performance appraisal strategy was essential to eliminate training data as a system. The fuzzy logic was to substantially control the energy transfer system under the active variation of the parameter system. Nevertheless, in decision-making, the management ability of these cognitive systems was a fuzzy neural network to the hybrid learning system. In contrast, the highest deficiency of the conventional ambiguous neural network need for assistance as its critical network assembly was imperfect due to the dominance of static problems. These disadvantages have provoked to do this study.

Modeling of Proposed Method

These sections refer to the established MPPT system of the WECS. Velocity Energy Variation The importance of the established method is the method of enhancing the controlled energy at the maximum energy point of the wind speed. Furthermore, maximal aerodynamic efficiency is attained by making better utilize of wind power to helps track controllers. An essential technique of the power circuit is the connection of PMSG-driven wind turbine connected via an ac-dc-ac alteration system [25]. The permanent magnet synchronous generator is

associated with the AC phase through the abandoned rectifier circuit and the DC connection is related to the control of the inverter. The WECS through proposed MPPT technique has been described in the following Fig. 1. To accomplish that MPPT of WECS is described as below.

Wind Turbine Modeling

Wind turbine is converted wind speed as mechanical energy generated by generator’s wind turbine axis [19], this is specifies in Eq. (1).

$$P_m = \frac{1}{2} \rho A C_p(\lambda, \beta) V_\omega^3 \tag{1}$$

here, P_m refers WT mechanic output power, ρ refers density of air, A refers area swept via blades, V_ω refers wind speed on m/s , β refers pitch angle on degree, $C_p(\lambda, \beta)$ denotes wind turbine power co-efficient[2], the power coefficient is exhibited in Eq. (2).

$$C_p = 0.73 \left(\frac{151}{\lambda_i} - 0.58\beta - 0.002\beta^{2.14} - 13.2 \right) e^{-18\lambda_i} \tag{2}$$

(where) $\lambda_i = \left(\frac{1}{\lambda - 0.002\beta} - \frac{0.003}{\beta^2 + 1} \right)^{-1}$

C_p denotes on linear function of Tip Speed Ratio λ as well as pitch angle β . To utilize Eq. (2), maximal power may extract with respect to optimal tip speed ratio value. This is exhibited in eq. (3).

$$\lambda = \frac{\omega_r r}{V_\omega} \tag{3}$$

where r specifies tip radius of wind turbine blade, ω_r specifies turbine speed.

PMSG Modeling

Three phases is employed: wind generator changes, mechanic energy, electric energy. At this time, electrical torque (T_e) and mechanic torque (T_m) is mentioned [16, 23] at below eq. (4) and (5).

$$T_m = \frac{P_m}{\omega_r} \tag{4}$$

$$T_e = \frac{P_e}{\omega_e} = \frac{2}{p} \frac{P_e}{\omega_r} \tag{5}$$

here, ω_e implies electrical angular frequency, p implies poles count. Energy produced is linked to grid through rectifier, power circuit inverter. The switches of inverter have regulated through MPPT approach. The inputs are deemed as dc voltage of rectifier output, output current, time.

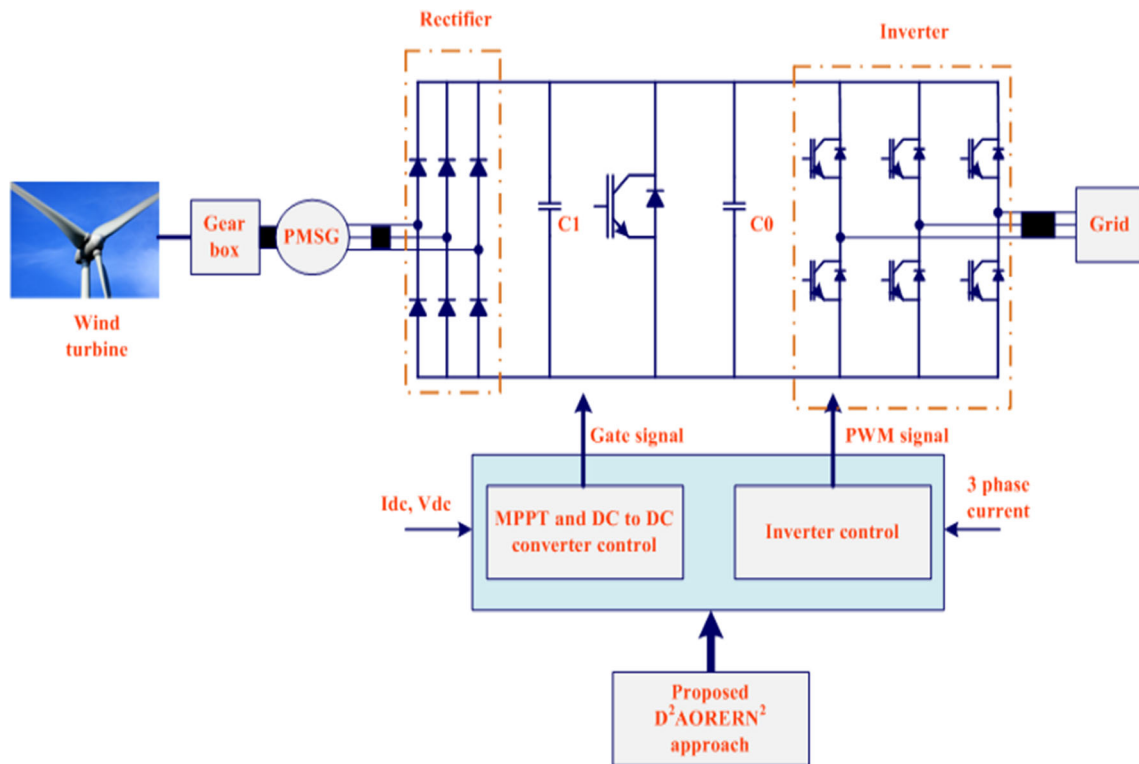


Fig. 1 Schematic diagram of proposed D²AORERN² approach for maximum power tracking in WECS

Implementation of Proposed D²AORERN² Approach

The proposed system creates reference dc voltage (V_{ref}) using the parameters of input from dc voltage (V_{dc}), dc current (I_{dc}), time (k). The output generation process of proposed D²AORERN² approach is clarified in Fig. 2.

DDAO Based Training Dataset Generation

This section describes the training dataset generation that means bio-inspired metaheuristic algorithm, such as Dynamic Differential Annealed Optimization (DDAO) [24]. DDAO approach is the meta-heuristics approach which imitates the method of creating high-quality steel. To produce the dual phase steel with high quality is the major concern for steel industry. The DDAO approach is the combined approach of random search, differential evolution, and simulated annealing. The minimum function is obtained in superior manner in this DDAO approach. The approach is chaotic as well as size of population is independent. Advanced high strength steel is dual-phase steel which provide wonderful mechanical characteristics. The annealing system is required for the production of these steel. In which, DDAO is applied to define the MPPT training dataset of radial basis function that is accomplished by proposed method, which means reduction of

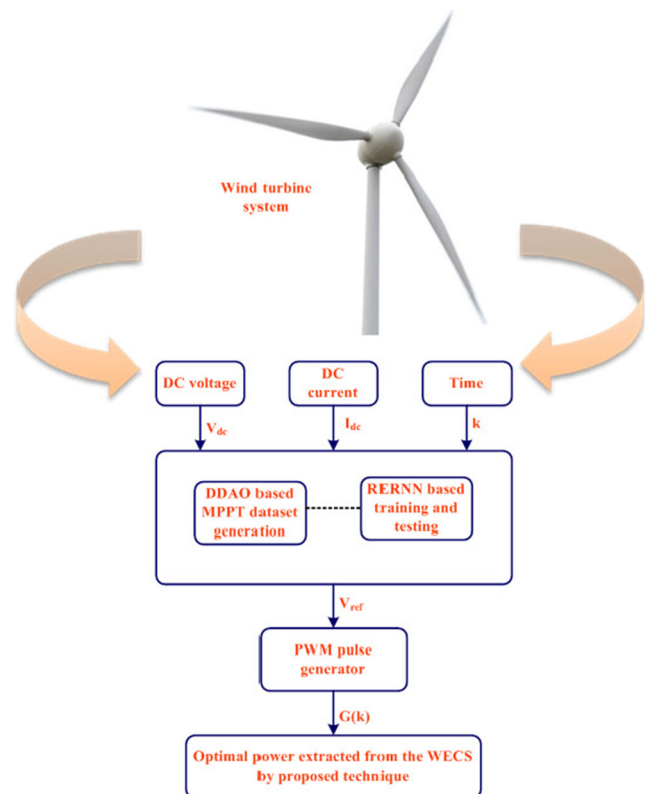


Fig. 2 Output generation process of proposed D²AORERN² approach

variation among the present and prior dc power. DDAO has the input of rectifier dc voltage output, output current, time. The output of DDAO is reference dc voltage, which is determined through MPPT. The input agents include dc voltage, dc current, time,

$$X_i^d = [(V_{dc1}, I_{dc1}, k_1)^1, (V_{dc2}, I_{dc2}, k_2)^2, (V_{dc3}, I_{dc3}, k_3)^1 \dots (V_{dcn}, I_{dcn}, k_n)^n] \tag{6}$$

Let, $(V_{dci}, I_{dci}, k_i)^d = X_i^d$ express the location of i^{th} agent at d^{th} dimension. For necessary n dimensions search space, the dc voltage is randomly generated. Random generator agents are expressed as,

$$V_{dc}^i = \begin{bmatrix} V_{11} & V_{12} & \dots & V_{1n} \\ V_{21} & V_{22} & \dots & V_{2n} \\ \vdots & \vdots & \vdots & \vdots \\ V_{n1} & V_{n2} & \dots & V_{nm} \end{bmatrix} \tag{7}$$

Objective function may be computed from agents. The necessary objective function is given by next relation (8).

$$\Phi = \text{Min}\{P_k - P_{k-1}\} \tag{8}$$

where P_k refers present time dc power and P_{k-1} refers earlier time dc power

(a). **Steps to get training dataset**

- Step 1. The first step of DDAO is the parameter initialization; here the input parameters like line voltage, line current, source voltage, and source current are initialized. Then the initialized populations are evaluated.
- Step 2. The evaluated parameters are sorted and randomly created that population.
- Step 3. After computing the fitness value, the better search agent is discovered.
- Step 4. The sub population is initialized and then evaluated that population and determine the best sub population.
- Step 5. The cooling operation is determined by,

$$C^k = (C_i - C_j) + C_R * F \tag{9}$$

here novel solution of repetition number k is represented as C^k , randomly selected solutions as population through random indices i, j is represented as C_i, C_j respectively, solution population is represented as C_R , forging parameter is indicated as F .

Step 7. The annealing process is done through the following equation by using the simulated annealing method,

$$P_n = e^{\frac{\Delta e}{T}} \tag{10}$$

$$\Delta e = \frac{S(C^k) - S(C^l)}{S(C^l)} \tag{11}$$

here probability of tolerant novel solution is specified as P_n , distinction among the intention value of proposed solution is specified as Δe , population size is specified as l . Determine the best value from the above equation.

- Step 8. If termination criteria is fulfilled, then the algorithm stops. Or move step 3.
- Step 9. Redo the better optimal solution is achieved.
- Step 10. Find the reference dc voltage (V_{ref}) from the best solution with the help of given MPPT rules [17].

- If $P_k \geq P_{k-1}$ and means $V_{dck} \geq V_{dc(k-1)}$; raise dc reference voltage need upgraded through ΔV_{dc} .
- If $P_k \geq P_{k-1}$ and means $V_{dck} < V_{dc(k-1)}$; raise dc reference voltage need degraded through ΔV_{dc} .
- If $P_k < P_{k-1}$ and means $V_{dck} \geq V_{dc(k-1)}$; raise dc reference voltage need upgraded through ΔV_{dc} .

If $P_k < P_{k-1}$ and means $V_{dck} < V_{dc(k-1)}$; raise dc reference voltage need upgraded through ΔV_{dc} .

The reference dc voltage may explain at next Eq. (10).

$$V_{refk} = V_{ref(k-1)} + \Delta V_{dc} \tag{12}$$

(where) $\Delta V_{dc} = \frac{P_k - P_{k-1}}{\text{slope}_k - \text{slope}_{k-1}}$

Step 9. Termination criteria.

If completed the termination criterion, then DDAO set for delivering the training dataset to RERNN. Training data set is trained the RERNN that is briefly explained in next section. Structure of DDAO technique is depicted in Fig. 3.

V_{ref} Prediction Using RERNN

RERNN is one of the artificial Neural Network that is employed in the field of mathematical modeling by utilizing the radial function. RERNN have six layers with selective memory property, but the Elman recurrent neural network has three layers. Figure 10 displays the structure of RERNN. The levels of RERNN are input layer, state layer, memory layer, sum layer, hidden, delay, output layer. The input of system is given to the input node and additionally, it accepts the output of the hidden layer with delay function. The previous outcome of sum layer and current outcome of state layer is accommodated by memory layer. To calculate the size of the previous sum layer information for next stage is major function of memory layer. Sum layer provides that function of summation which can add the present input, final recurrent hidden

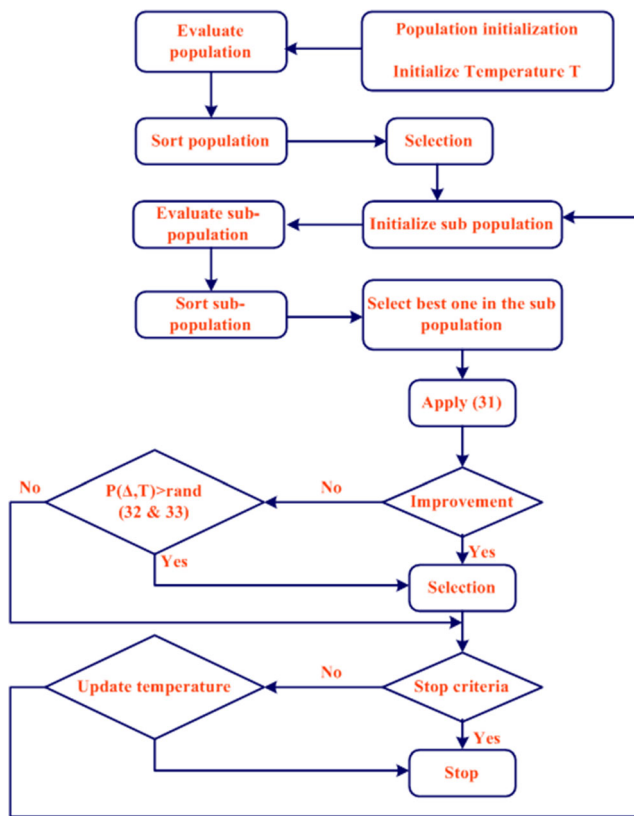


Fig. 3 Structure of DDAO technique

outcome as well as the result of memory layer [15]. The final probabilistic value of the output layer is obtained by the hidden layer. The current hidden layer output is propagated back by the delay layer. Conjugate gradient descent algorithm, generalized Armijo search approaches are used in this RERNN approach and the output is depending on these two approaches.

Step 1. Initialization

Initially, the nodes number, iteration, weight vector $m_e = [m_1, m_2, \dots, m_n]$, and the count of hidden nodes.

Step 2. Random Generation

Input parameters are generated random through the random vector.

Step 3. Output calculation

The error value is determined by,
 $E_k(n) = y_k(n) - \hat{y}_k(n), k = 1, 2, \dots, L.$
 where, $\hat{y}_k(n)$ refers desired output vector of it neuron in output, $y_k(n)$ as output vector of ith neuron in output layer

Step 4. Check the iteration is maximum

The data is processed when the iteration is less than the maximum iteration otherwise stop the process.

Step 5. Learning Rate Determination

Generalized Armijo search approach is utilized to determine the learning rate by using the following condition,

$$e(m^k + L_R P^k) \leq e(m^k) + \alpha_1 L_R e_w^k (P^k)^t, \alpha_1 \geq 0 \tag{13}$$

Step 6. New Weight Determination

Gradient descent algorithm is utilized to determine the new weight which is articulated as,

$$m^{k+1} = m^k + L_R P^k \tag{14}$$

Step 7. Check the Maximum Iteration

If the iteration is reached then stop the process. Or else maximize that repetition and goes step 6.

Step 8. Determine the Direction

The direction of the learning process is calculated by using the conjugate gradient descent algorithm which is expressed as,

$$P^k = -e_w^k + \beta P^{k-1} \tag{15}$$

$$\beta = \frac{\alpha e_w^k (P^{k-1})^t}{P^{k-1} (P^{k-1} - e_w^k)}, \alpha \in (0, 1) \tag{16}$$

Step 9. Calculate the overall error

The overall error is computed by,

$$E_T = \sum_{n=1}^I \sum_{k=1}^N y_{nk} - \hat{y}_{nk}$$

Step 10. Repeat process

Repeat the procedure from step 2 until entire error is lower than preferred error.

If done the procedure, then the RERNN presents reference dc side voltage. This voltage converts as necessary inverter control pulses. Then go to the step 3. Again repeat the process until obtain the best outcome. Structure of RERNN technique is explained at following Fig. 4.

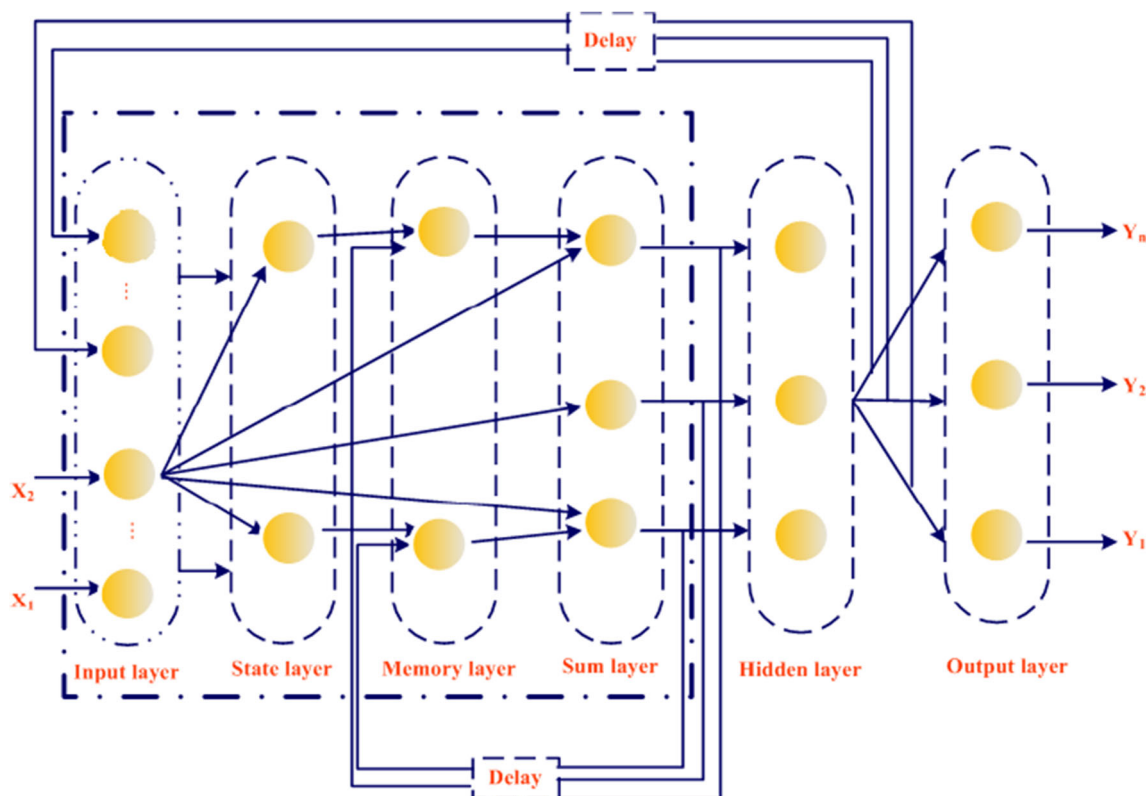


Fig. 4 Structure of RERNN technique

Results with Discussion

The proposed approach is activated in MATLAB/Simulink. The hybrid MPPT search system depends on WECS is represented in

Fig. 5. The designing of WECS is depicted in Fig. 6. The execution parameter is mentioned in Table 1. During testing time, RERNN is trained to dataset and presents reference dc side voltage. The $D^2AORERN^2$ method is examined with 2 different case

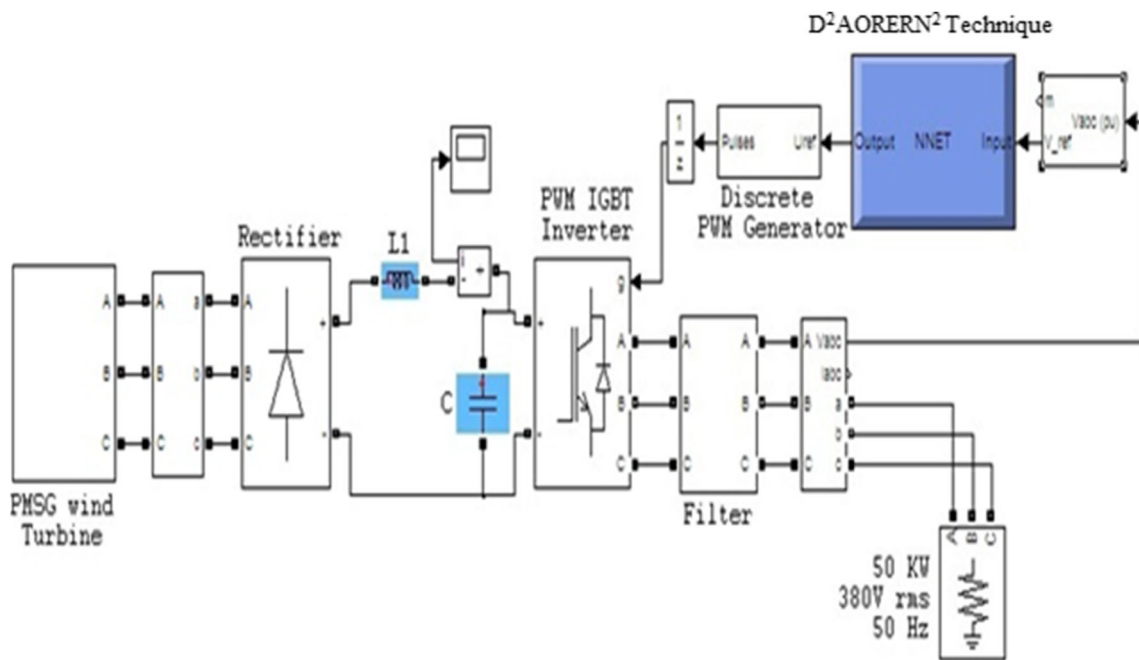


Fig. 5 Structure of WECS using proposed system

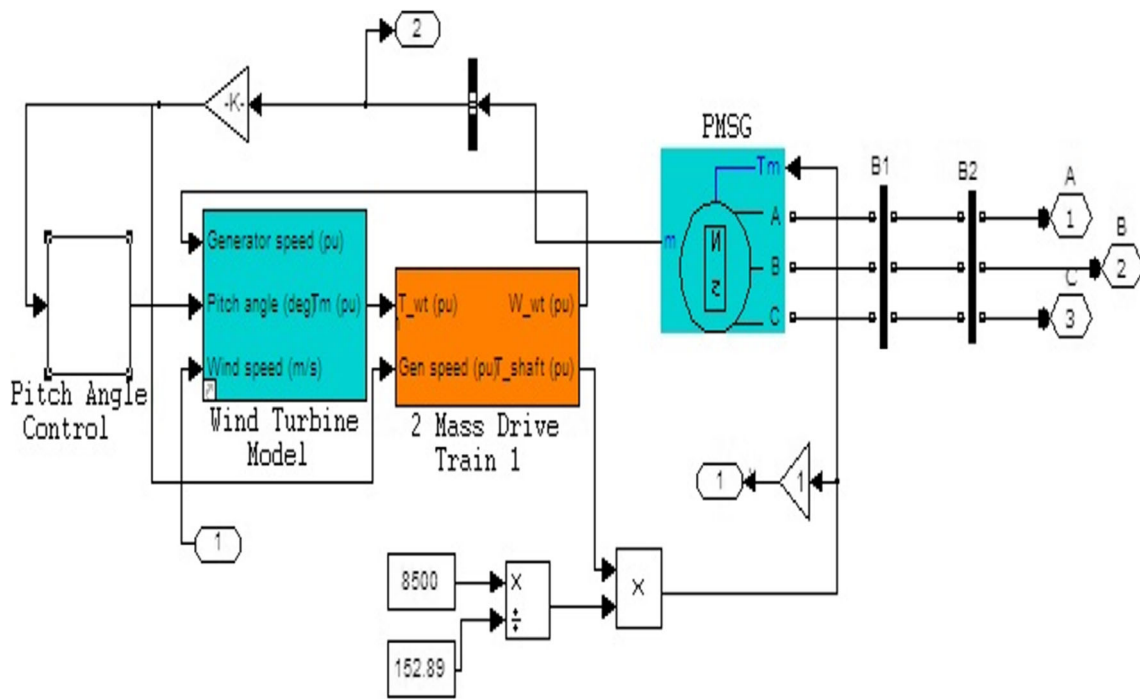


Fig. 6 Wind energy conversion system framework

studies and its efficiency is compared with existing techniques, viz. genetic algorithm (GA), particle swarm optimization (PSO), Hill Climb Search (HCS).

The wind speed is unspecified as stable that is, 8 m / s. Figure 7 displays the wind speed. The execution of usual time analysis refers $T_s = 0.5$ s. Figures 8 and 9 shows the inverter voltage with current for the single phase. At 0 to 0.22 s, the voltage stable wind profile of inverter phase A is changed from 0 to 399 V. In the time of 0 to 0.22 s, the current stable wind profile of inverter phase A is changed from 0 to 78A. The dc connection voltage for stable wind profile is depicted in Fig. 10. At 0 to 0.2 s, the dc connection voltage for stable wind profile is changed from 0 to 440 V, at 0.2 to 0.5 s the dc connection voltage for stable wind profile is varied from 440 V to 380 V.

Figure 11 represents the permanent magnet synchronous generator rotor speed depends upon input wind speed. The

rotor speed on constant wind profile at the time interval 0 to 0.2 s, the value is varied from 0 to 140rps and the time instant of $t = 0.2$ to 0.5 s, the rotor speed value is changed from 140rps to 130rps. The rotor reaches maximal speed at 0.2 s and moves at stable speed. The real power of stable wind profile explained at Fig. 12. Real power to constant wind profile is changed from 0 to 4500 W at time interval 0 to 0.2 s. At time interval $t = 0.2$ s to 0.5 s, real power value changed to 4500 to 3800 W. The efficiency of $D^2AORERN^2$ technique is examined subject to given 2 case studies.

Case (I): Step Variation of Wind System This section describes the efficiency of $D^2AORERN^2$ method. Figure 13 portrays the input wind profile. Here, the input wind variation is implemented. Figures 14 and 15 displays the inverter voltage with current using $D^2AORERN^2$ method. Here, the proposed method efficiently monitors the MPPT decreased time delay.

Table 1 Parameter execution

Parameter	Value
Stator resistance (R_s)	1.5Ω
Stator inductance (L_d, L_q)	0.01 mH
Flux induced to magnets (φ)	0.1194wb
Inertia moment (J)	2 kg m
Count of poles (P)	4
Frequency switching (f_s)	20 KHz
Rotor radius (r)	1.525 m

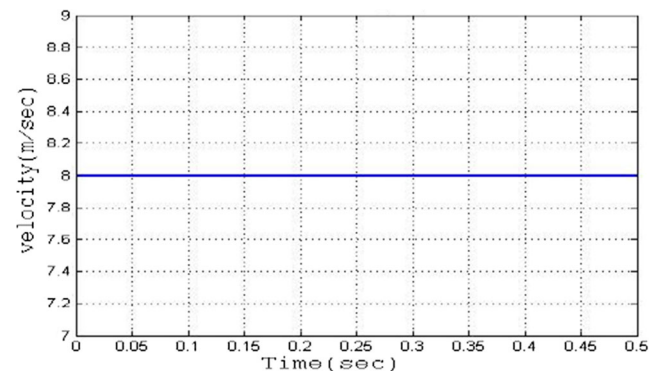


Fig. 7 Wind velocity of stable wind system

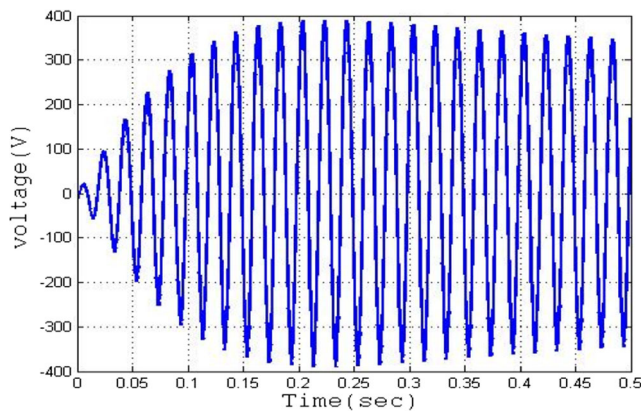


Fig. 8 Inverter phase A voltage stable wind system

Inverter phase A voltage value is changed from the time interval 0.25 to 0.5 s is 290 V. Inverter phase A current value is changed from time interval 0.25 to 0.5 s is 80A. Figure 16 implicates the voltage of dc connection capacitor with proposed technique. Here, the dc connection voltage of D²AORERN² system is varied at time interval t = 0 to 0.25 s and the value is varied between 0 to 450 V. By then the time variation of t = 0.25 to 0.5 s then the value for the DC link voltage is varied between 450 to 290 V. Figure 17 dis-

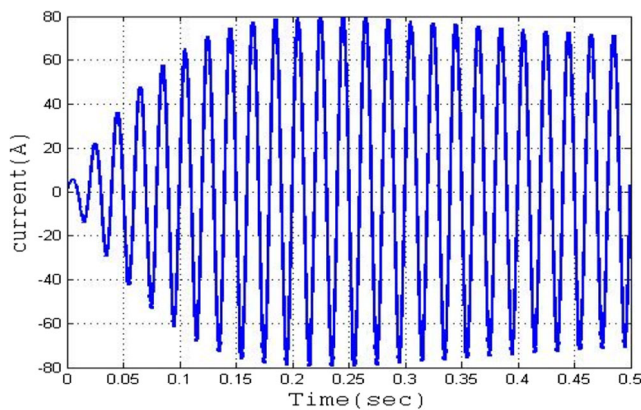


Fig. 9 Inverter phase A current stable wind system

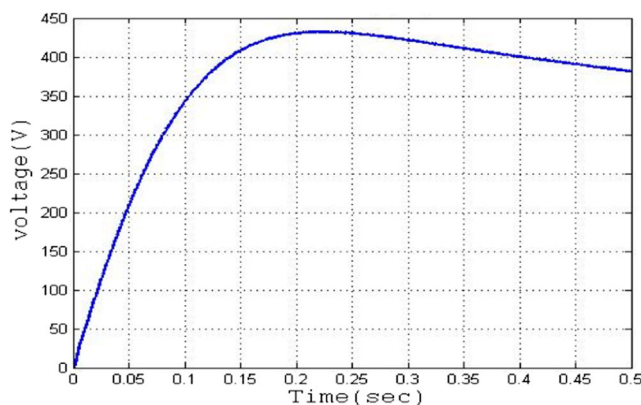


Fig. 10 DC link voltage stable wind system

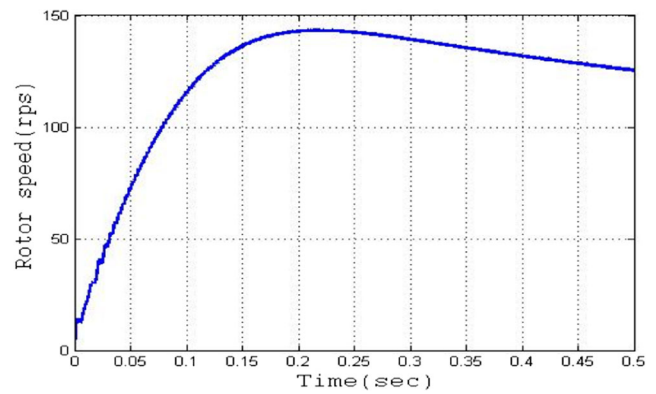


Fig. 11 Rotor speed of stable wind system

plays PMSG rotor speed utilizing D²AORERN² technique depending on input step wind. The rotor speed of the proposed technique is varied at the time interval t = 0 to 0.25 s and value is varied between 0 to 145rps. By then the time variation of t = 0.25 to 0.5sec then the value for the rotor speed is varied between 145rps to 80rps.

Figure 18 shows the system's real power with D²AORERN² method. The real power of D²AORERN² technique is varied at the time interval t = 0 to 0.25 s and its value

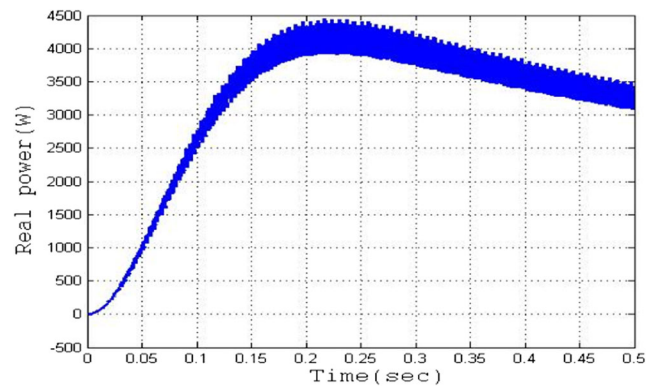


Fig. 12 Real power to stable wind profile

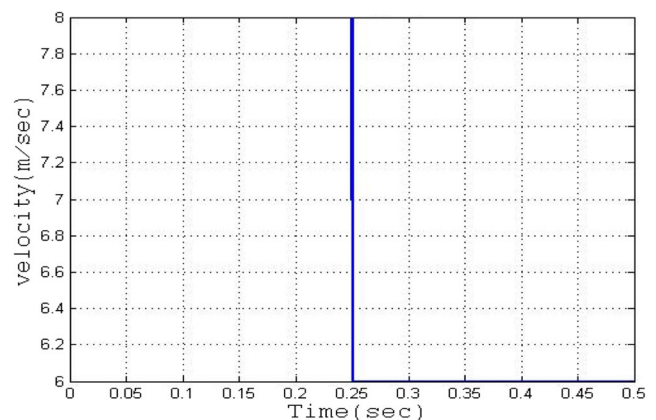


Fig. 13 Wind velocity of stable wind profile

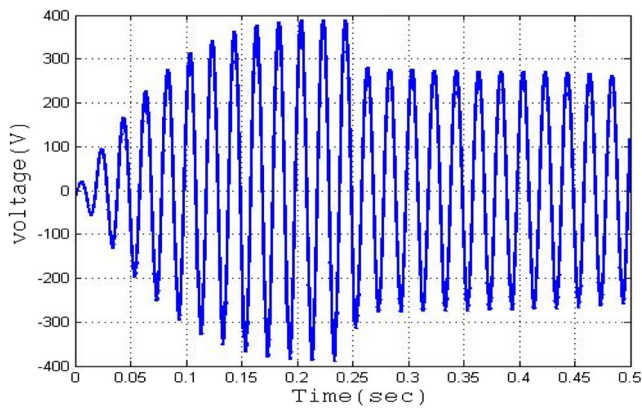


Fig. 14 Voltage of inverter phase A for $D^2AORERN^2$ system

is 0 to 4400 W and the time interval $t = 0.25$ to 0.5 the real power value is 4400 to 1800 W. Figures 19 and 20 shows the inverter voltage with current comparison. Here, the HCS system is monitored the MPPT based on pitch change at 0.28 s. The voltage with current amplitude achieves 130 V, 30 A through the step changes period of application. PSO monitors the maximal voltage with current amplitude on 6 m / s wind speed attains 210 V, 44 A at the time duration 0.02 s. The proposed system tracks the maximal voltage amplitude with current in 6 m / s wind speed attains 280 V, 58 A in the absence of delay. Figure 21 displays the real power of 3 systems. Here,

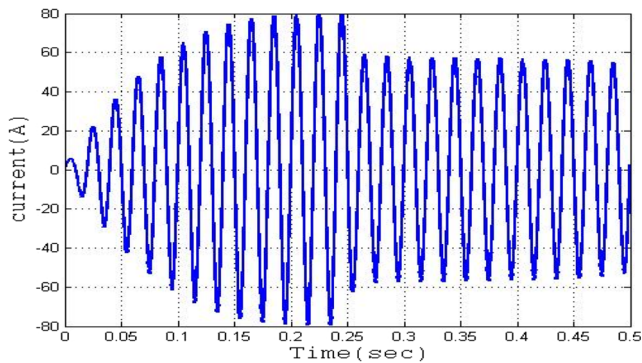


Fig. 15 Current of inverter phase A for $D^2AORERN^2$ system

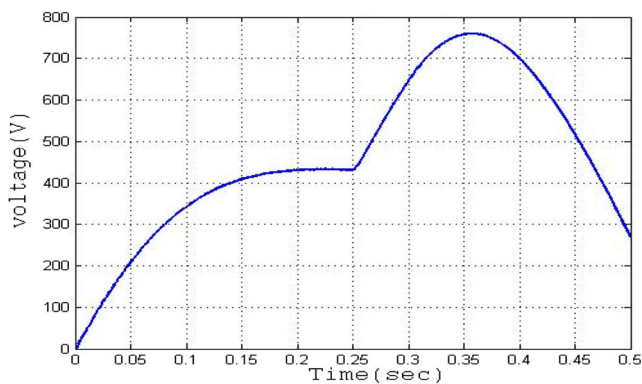


Fig. 16 DC connection voltage for $D^2AORERN^2$ system

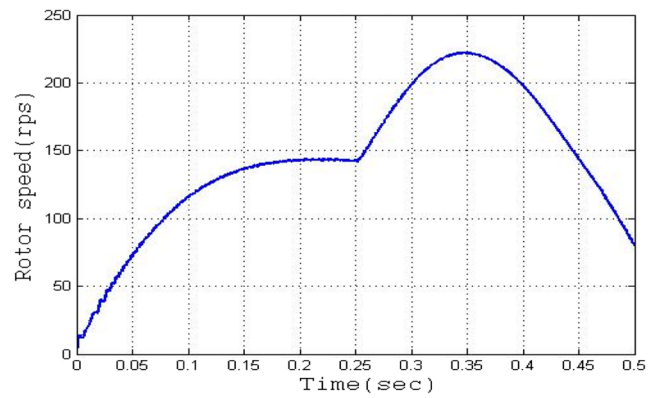


Fig. 17 Rotor speed of $D^2AORERN^2$ system

the PSO monitored the maximal power in 6 m / s input wind speed represents 1400 W through the time delay of 0.02 s. The proposed system contains 4500 W power in 8 m / s wind speed input, also track the maximum power through 6 m / s wind speed is 2300 W in the absence of delay. The results prove that

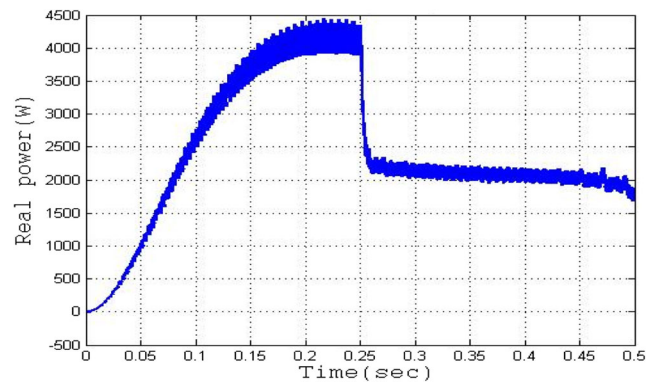


Fig. 18 Real power of $D^2AORERN^2$ system

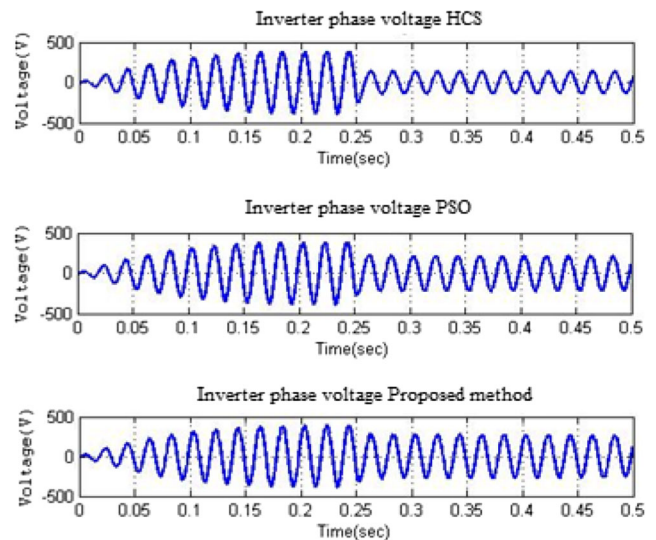


Fig. 19 Voltage of inverter phase A comparison

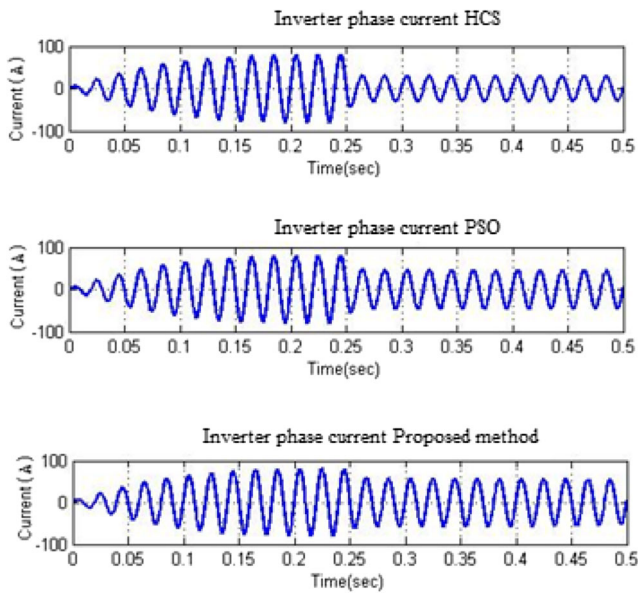


Fig. 20 Current of inverter phase A comparison

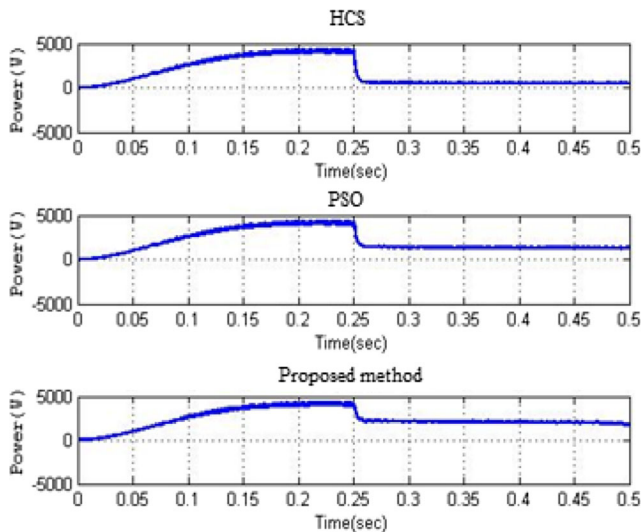


Fig. 21 Comparison of real power

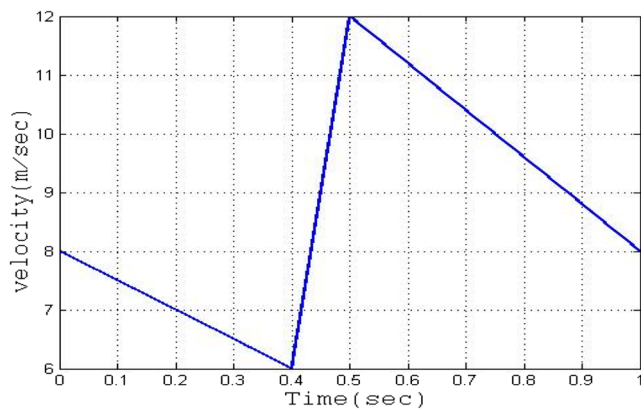


Fig. 22 Wind velocity of stable wind system

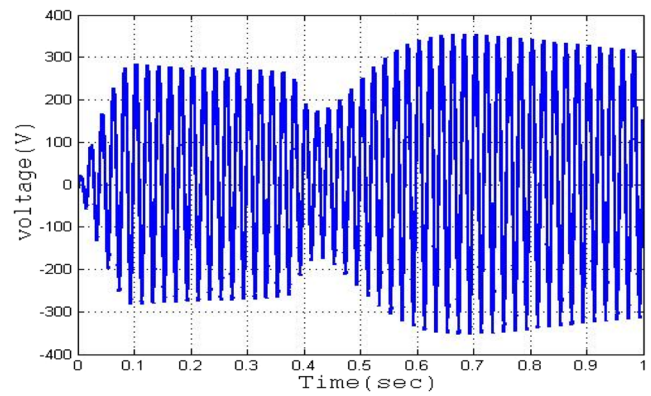


Fig. 23 Voltage of inverter phase A for D²AORERN²system

the D²AORERN² is proficiently tracking maximal power point at step variation of wind system.

Case (ii): Ramp Variation of Wind Profile This is evaluated at simulation time $T_s = 1$ s. The wind system attains 8 m/s in initial interval, it diminished with 6 m/s at 0.4 s, again maximized to 12 m/s in 0.5 s, lastly diminished at 8 m/s. Figure 22 implicates the variation of the wind profile ramp. This variation is used to proposed system and outcomes are

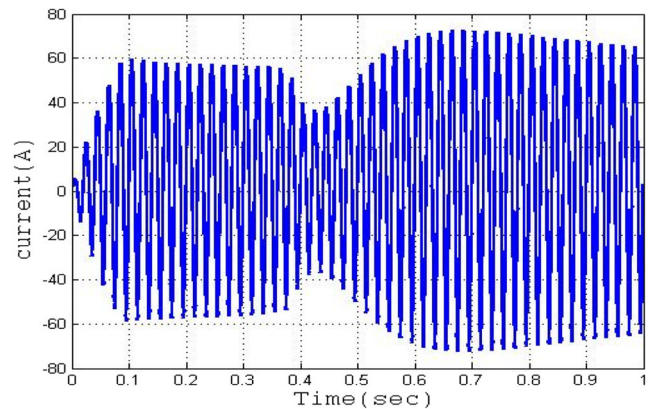


Fig. 24 Current of inverter phase A for D²AORERN²system

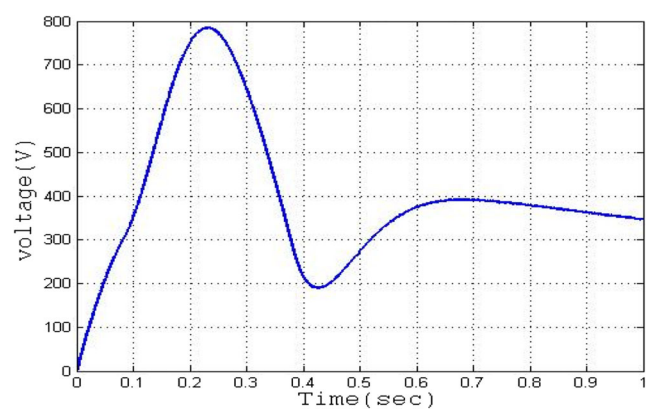


Fig. 25 DC connection voltage of D²AORERN²system

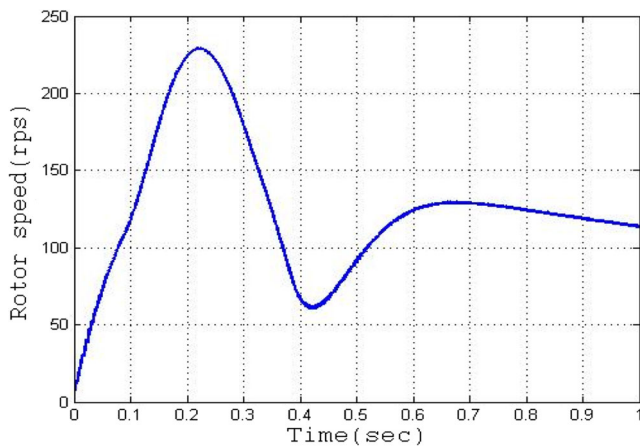


Fig. 26 Rotor speed of $D^2AORERN^2$ system

evaluated below. Figures 23 and 24 depict the inverter voltage with current utilizing $D^2AORERN^2$ method. Here, $D^2AORERN^2$ system successfully monitors the MPPT using decreased delay of time. The dc link voltage across capacitor utilizing $D^2AORERN^2$ technique is implicated in Fig. 25. It

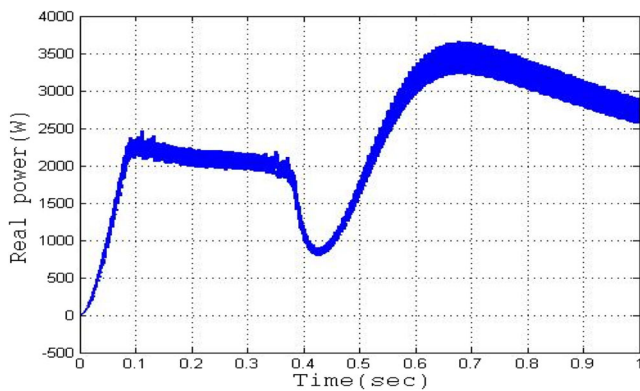


Fig. 27 Real power of $D^2AORERN^2$ system

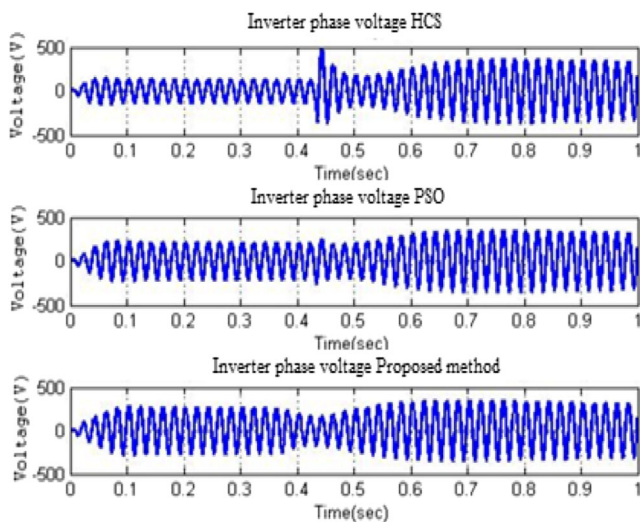


Fig. 28 Inverter phase A voltage comparison

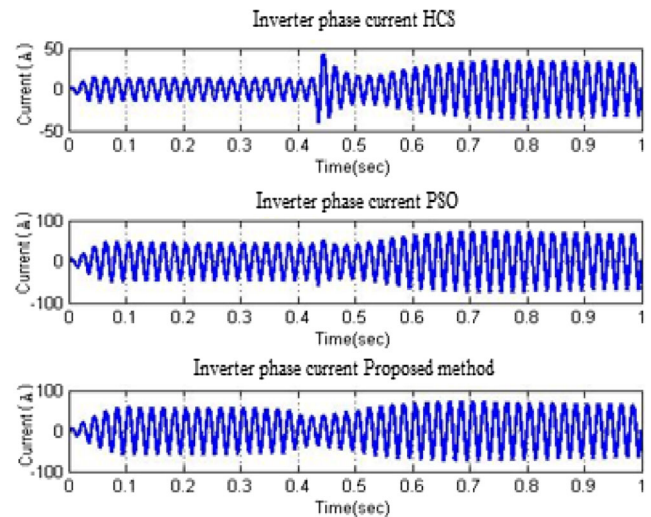


Fig. 29 Inverter phase A current comparison

presents an enhanced voltage profile likened with previous models. The speed of permanent magnet synchronous generator rotor using $D^2AORERN^2$ system is portrayed in Fig. 26. The real power utilizing $D^2AORERN^2$ system is depicted in Fig. 27.

The PSO with dc voltage on capacitor is shown in Fig. 28. Here, the capacitor does not perform the enhanced voltage profile based on permanent magnet synchronous generator rotor speed, voltage, current variation. Figure 29 represents the variation of permanent magnet synchronous generator rotor speed with PSO system. Figure 30 specifies the real power comparison.

After the inverter voltage with current of 3 systems are represented in Figs. 28 and 29 respectively. Here, HCS contains 180 V voltage, 18A current. PSO monitors the maximal voltage amplitude with current in 6 m / s indicates 310 V, 74A using time interruption 0.2 s. The $D^2AORERN^2$ system monitors the maximal amplitude of voltage with current in wind speed of 6 m / s denoting 330 V and 78 A. It displays that the

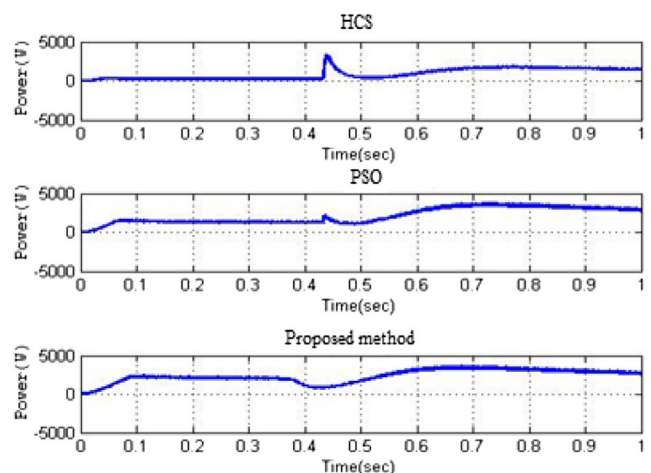


Fig. 30 Real power comparison

Table 2 Confusion matrix of D²AORERN² approach

Kinds of fault	True positive	True negative	False positive	False negative	Accuracy	Sensitivity	Specificity
Case 1	2	12	0	2	0.95	0.62	0.90
Case 2	3	11	1	2	0.95	0.66	0.89

Table 3 Quality of Solution comparison

Various optimization models	Best fitness	Worst fitness	Mean fitness	Standard deviation	Coefficient of variation	Error of best
D2AORERN2	1,110,946.01	1,297,382.12	1,407,656.56	2051.98	7.075	0.82
HCS	1,105,353.97	1,194,932.90	1,305,205.43	3072.12	9.09	0.10
PSO	1,105,268.87	1,064,197.09	1,293,894.48	4216.80	9.75	1.27
GA	1,105,343.97	1,046,828.14	1,198,634.82	11,771.84	8.89	0.32

HCS system primarily monitors the maximal power of 3400 W in wind speed of 8 m/s at 0.5 s. It cannot obviously monitors that maximal power of 6 m/s. The 12 m/s contains 1600 W power using time delay of 0.3 s along with power satisfies the lessening at simulation time. PSO monitors the maximal power of 8 m/s wind speed input is 2000 W using time delay of 0.45 s. It has 1000 W actual power of 6 m/s wind speed input; actual power value indicates 3600 W through wind speed in 12 m/s at time delay of 0.24 s. The time interval 0.74 s to the simulation time of actual power value decreased. Obviously it portrays established technique consists of 2600 W of power in 8 m/s wind speed input which diminished to 1000 W in 6 m/s wind speed using time delay of 0.02 s. It reaches a maximal power of 3700 W at wind speed input of 12 m/s using time delay of 0.16 s.

Table 2 tabulates the confusion matrix of D²AORERN² system. Here, true positive (TP), true negative (TN), false positive (FP), false negative (FN) are analyzed. TP allocates correctly labelled positive signals. TN correctly labelled negative signals. FP is wrongly labelled negative signals. FN is wrongly labelled positive signals,

$$accuracy = \frac{TP + TN}{TP + TN + FN + FP} \tag{17}$$

$$precision = \frac{TP}{FP + TP} \tag{18}$$

Table 4 Efficiency of proposed and existing techniques

Solution Technique	Efficiency (%)
D2AORERN2	99%
HCS	89%
PSO	85%
GA	81%

$$recall \text{ (or) specificity} = \frac{TP}{FN} TP \tag{19}$$

$$sensitivity = \frac{TN}{FP} TN \tag{20}$$

If positive the sensitivity value, the parameters assumes true positive fraction. If negative the specificity value, the parameters assumes true negative fraction of system secure in transmitting line outages states and generator outages with the help of D²AORERN² method. Table 3 tabulates the comparison of Quality of Solution (QoS). Here, the parameters, viz. best, worst, mean fitness, standard deviation, coefficient of variation, error of best are examined. Table 4 displays the efficiency of proposed and existing method. The comparison outcomes prove that the D²AORERN² method attains better MPPT in various kinds of the variation of wind profile.

Conclusion

In this article, a hybrid D²AORERN² approach is proposed to monitor the maximum power of wind energy conversion system. Here, training dataset depending on MPPT is found with DDAO algorithm. Based on training dataset, RERNN is trained. The experimental shows that the reference dc voltage rectifier is transformed for controlling the inverter switch pulses. The merits of D²AORERN² method are good searching ability, maintain system stability and attain desired performance through parameter uncertainties. The D²AORERN² technique is compared with GA, PSO and HCS technique to validate the efficiency. The outcomes prove that the D²AORERN² technique is most effectual technique than existing methods for achieving WECS maximum power during parameter uncertainties. In case 1, the TP, TN, FP, FN, accuracy, sensitivity and specificity of

D^2 AORERN² technique is 2, 12, 0, 2, 0.95, 0.62 and 0.90. In case 2, the D^2 AORERN² technique attains 2, 11, 1, 2, 0.95, 0.66 and 0.89.

Funding This research did not receive any specific grant from funding agencies in the public, commercial, or not-for-profit sectors.

Data Availability Statement Data sharing does not apply to this article as no new data has been created or analyzed in this study.

Code Availability Not applicable.

Declarations The authors declare that they have no known competing financial interests or personal relationships that could have appeared to influence the work reported in this paper.

Conflict of Interest Authors declare that they have no conflict of interest.

Ethical Approval This article does not contain any studies with human participants performed by any of the authors.

Consent to Participate Not applicable.

References

- Abdullah MA, Yatim AH, Tan CW, Saidur R (2012) A review of maximum power point tracking algorithms for wind energy systems. *Renew Sust Energy Rev* 16(5):3220–3227
- Adžić EM, Porobić VB, Adžić MS, Ivanović ZR (2016) Advanced induction motor drive control with single current sensor. *Thermal Science*. 20(2):421–436
- Agarwal V, Aggarwal RK, Patidar P, Patki C (2009) A novel scheme for rapid tracking of maximum power point in wind energy generation systems. *IEEE Trans Energy Convers* 25(1):228–236
- Alzayed M, Chaoui H, Farajpour Y (2021) Maximum power tracking for a wind energy conversion system using Cascade-forward neural Networks. *IEEE transactions on sustainable energy*.
- Azzouz M, Elshafei AL, Emara H (2011) Evaluation of fuzzy-based maximum power-tracking in wind energy conversion systems. *IET Renew Power Gen* 5(6):422–430
- Banik R, Das P, Ray S, Biswas A (2020) Wind power generation probabilistic modeling using ensemble learning techniques. *Mat Today: Proceed* 26:2157–2162
- Calderaro V, Galdi V, Piccolo A, Siano P (2008) A fuzzy controller for maximum energy extraction from variable speed wind power generation systems. *Electric. Power Syst Res* 78(6):1109–1118
- Chen CH, Hong CM, Cheng FS (2012a) Intelligent speed sensorless maximum power point tracking control for wind generation system. *Int J Electr Power Energy Syst* 42(1):399–407
- Chen J, Chen J, Gong C (2012b) Constant-bandwidth maximum power point tracking strategy for variable-speed wind turbines and its design details. *IEEE Trans Ind Electron* 60(11):5050–5058
- Chen J, Chen J, Gong C (2012c) New overall power control strategy for variable-speed fixed-pitch wind turbines within the whole wind velocity range. *IEEE Trans Ind Electron* 60(7):2652–2660
- Cirincione M, Pucci M, Vitale G (2012) Growing neural gas-based mppt of variable pitch wind generators with induction machines. *IEEE Trans Ind Appl* 48(3):1006–1016
- Dalala ZM, Zahid ZU, Lai JS (2013) New overall control strategy for small-scale WECS in MPPT and stall regions with mode transfer control. *IEEE Trans Energy convers* 28(4):1082–1092
- Dang DQ, Wang Y, Cai W (2012) Offset-free predictive control for variable speed wind turbines. *IEEE. Trans Sustain Energy* 4(1):2–10
- Eltamaly AM, Mohamed MA, Abo-Khalil AG (2021) Maximum power point tracking strategies of grid-connected wind energy conversion systems. *Control Oper Grid-Connected Wind Energy Syst* 193–225.
- Gao T, Gong X, Zhang K, Lin F, Wang J, Huang T, Zurada JM (2020) A recalling-enhanced recurrent neural network: conjugate gradient learning algorithm and its convergence analysis. *Inf Sci* 519:273–288
- Ghafil HN, Jármai K (2020) Dynamic differential annealed optimization: new metaheuristic optimization algorithm for engineering applications. *Appl Soft Comput* 93:106392
- Hong CM, Ou TC, Lu KH (2013) Development of intelligent MPPT (maximum power point tracking) control for a grid-connected hybrid power generation system. *Energy*. 50:270–279
- Kazmi SM, Goto H, Guo HJ, Ichinokura O (2010) A novel algorithm for fast and efficient speed-sensorless maximum power point tracking in wind energy conversion systems. *IEEE Trans Ind Electron* 58(1):29–36
- Kesraoui M, Korichi N, Belkadi A (2011) Maximum power point tracker of wind energy conversion system. *Renew Energy* 36(10):2655–2662
- Khan MJ (2021) An AIAPO MPPT controller based real time adaptive maximum power point tracking technique for wind turbine system. *ISA Trans* 123:492–504
- Kot R, Rolak M, Malinowski M (2013) Comparison of maximum peak power tracking algorithms for a small wind turbine. *Math Comput Simul* 91:29–40
- Koutroulis E, Kalaitzakis K (2006) Design of a maximum power tracking system for wind-energy-conversion applications. *IEEE Trans Ind Electron* 53(2):486–494
- Le DA, Vo DN (2016a) Cuckoo search algorithm for minimization of power loss and voltage deviation. *Int J Energy Optim Eng (IJEEO)* 5(1):23–34
- Le DA, Vo DN (2016b) Cuckoo search algorithm for minimization of power loss and voltage deviation. *Int J Energy Optim Eng (IJEEO)* 5(1):23–34
- Lin WM, Hong CM (2010) Intelligent approach to maximum power point tracking control strategy for variable-speed wind turbine generation system. *Energy*. 35(6):2440–2447
- Lo KY, Chen YM, Chang YR (2010) MPPT battery charger for stand-alone wind power system. *IEEE Trans Power Electron* 26(6):1631–1638
- Mendis N, Muttaqi KM, Sayeef S, Perera S (2012) Standalone operation of wind turbine-based variable speed generators with maximum power extraction capability. *IEEE Trans Energy Convers* 27(4):822–834
- Mesemanolis A, Mademlis C, Kioskeridis I (2012) High-efficiency control for a wind energy conversion system with induction generator. *IEEE Trans Energy Convers* 27(4):958–967
- Mythili S, Thiyagarajah K, Rajesh P, Shajin FH (2020) Ideal position and size selection of unified power flow controllers (UPFCs) to upgrade the dynamic stability of systems: an antlion optimiser and invasive weed optimisation algorithm. *HKIE Trans* 27(1):25–37
- Pan CT, Juan YL (2009) A novel sensorless MPPT controller for a high-efficiency microscale wind power generation system. *IEEE Trans Energy Convers* 25(1):207–216
- Rajesh P, Shajin F (2020) A multi-objective hybrid algorithm for planning electrical distribution system. *Eur J Electrical Eng* 22(4–5):224–509
- Ramasamy BK, Palaniappan A, Mohamed Yakoh S (2013) Direct-drive low-speed wind energy conversion system incorporating

- axial-type permanent magnet generator and Z-source inverter with sensorless maximum power point tracking controller. *IET Renew Power Gen* 7(3):284–295
33. Samokhvalov DV, Jaber AI, Almahturi FS (2021) Maximum power point tracking of a wind-energy conversion system by vector control of a permanent magnet synchronous generator. *Russ Electr Eng* 92(3):163–168
 34. Shajin FH, Rajesh P. (2020). Trusted secure geographic routing protocol: outsider attack detection in mobile ad hoc networks by adopting trusted secure geographic routing protocol
 35. Thota MK, Shajin FH, Rajesh P (2020) Survey on software defect prediction techniques. *Int J Appl Sci Eng* 17(4):331–344
 36. Tonsing B, Vadhera S, Gupta AR (2021) Implementation of hill climb search algorithm based maximum power point tracking in wind energy conversion systems. In *advances in renewable energy and sustainable environment*, 191–199. Springer, Singapore.
 37. Vu V.P, Ngo V.T, Do V.D, Truong D.N, Huynh T.T, Do T.D (2021) Robust MPPT observer-based control system for wind energy conversion system with uncertainties and disturbance.
 38. Wang J, Bo D, Miao Q, Li Z, Wu X, Lv D (2021) Maximum power point tracking control for a doubly fed induction generator wind energy conversion system based on multivariable adaptive super-twisting approach. *Int J Electrical Power Energy Syst.* 124:106347
 39. Xia Y, Ahmed KH, Williams BW (2011) A new maximum power point tracking technique for permanent magnet synchronous generator based wind energy conversion system. *IEEE Trans Power Electronics* 26(12):3609–3620
 40. Xia Y, Ahmed KH, Williams BW (2012) Wind turbine power coefficient analysis of a new maximum power point tracking technique. *IEEE Trans Ind Electron* 60(3):1122–1132
 41. Zou Y, Elbuluk M, Sozer Y (2011) Stability analysis of maximum power point tracking (MPPT) method in wind power systems. In 2011 IEEE industry applications society annual meeting, 1–8. IEEE.

Publisher's Note Springer Nature remains neutral with regard to jurisdictional claims in published maps and institutional affiliations.